JOURNAL OF MATERIALS SCIENCE 27 (1992) 2670–2676

Binder chemistry, adhesion and structure of interfaces in thick-film metallized aluminium nitride substrates

C. E. NEWBERG
IBM Corporation, East Fishkill, NY 12533, USA

S. H. RISBUD
Division of Materials Science and Engineering and Materials Research Center, University of California, Davis, CA 95616-5294, USA

Aluminium nitride substrates from three different sources were metallized by standard thick film processing using gold conductor pastes, Pd–Ag paste, and a ruthenium oxide resistor paste. Screen printed pastes were fired in a typical three-zone furnace to obtain metallized AlN substrates. Interfacial reaction zones were studied by microscopic (optical and scanning electron microscopy) and electron beam microprobe analysis techniques. The elements in the binder materials in thick film pastes form amorphous phases at the interface which influence the adhesion of thick films to the AlN substrate. The lack of certain elements (Cd, Zn, Ca) in the binder of the gold thick-film paste led to weaker adhesion and severe degradation of the thick-film adhesion during thermal cycling.

1. Introduction

The almost exponential increase in density of components packaged in microelectronic circuitry has created a myriad of materials problems and opportunities in electronic packaging technology. Very large-scale integration (VLSI) and ultra large-scale integration (ULSI) monolithic chips present challenges for electronic packaging as they involve thermal stress management and heat removal problems associated with high power levels. Dielectric ceramic substrates with an appropriate combination of electrical and thermal properties are in various stages of development for high-speed, high-power microelectronic applications [1–6].

Several materials are at the forefront as potential replacements for the commonly used alumina (Al_2O_3) and beryllia (BeO) substrate materials. Silicon carbide (SiC) and aluminium nitride (AlN) are two recent substrate materials which have attractive thermal properties for packaging systems. In addition to having exceptionally high thermal conductivities, these materials have thermal expansion coefficients which closely match those of silicon and gallium arsenide. Silicon carbide (SiC), with a dielectric constant of ≈ 42 at 1 MHz, is considered to be of potential use in special microwave frequency applications. Far greater recent development effort has been directed toward aluminium nitride (AlN), including issues related to high thermal conductivity substrate sintering, development of metallization systems, and processing by co-firing.

We report here experimental work on the metallization of AlN substrates obtained from three different commercial sources. The substrates were fired after screen printing gold, Pd–Ag, and ruthenium oxide thick-film pastes. Interfacial reaction zones between the thick film and substrate were examined by optical microscopy, scanning electron microscopy (SEM), energy dispersive spectroscopy (EDS), and electron beam microprobe analysis. The effects of elements in the pastes on the adhesion of the thick film to AlN were also studied.

2. AlN in electronic packaging

The potential of aluminium nitride as an electronic packaging substrate is based mainly on the high thermal conductivity of pure AlN. Slack [3] reported the thermal conductivity of a single crystal of AlN to be $\approx 200\ W\,m^{-1}\,°C^{-1}$, although polycrystalline aluminium nitride has a thermal conductivity as low as $60\ W\,m^{-1}\,°C^{-1}$. The constraints on sintering AlN to near theoretical density, and obtaining pure single crystals, severely limit the realization of high thermal conductivity in AlN. Recent advances in using Y_2O_3 and other additives as sintering aids have promoted several efforts to manufacture aluminium nitride for electronic substrate applications. Iwase *et al.* [4] reported utilizing sheet-casting techniques to manufacture substrates made out of AlN with slight additions of Y_2O_3. Maya [7] has manufactured aluminium nitride powder with good purity by a synthetic approach, and Beauchamp *et al.* [8] have utilized hot pressing of shock-activated AlN to obtain dense discs. Kurokawa *et al.* [9] have recently examined the effect of CaC_2, CaO, Y_2O_3 and C on the thermal conductiv-

0022–2461 © 1992 Chapman & Hall

ity of hot-pressed aluminium nitride. They found that the addition of CaC_2 powder resulted in a thermal conductivity of $180\ \mathrm{W\,m\,K^{-1}}$. The CaC_2 helps increase the thermal conductivity by reacting with the oxygen left in the aluminium nitride, thus removing or reducing the thermal barriers caused by the oxygen impurities at the grain boundaries of the aluminium nitride [9].

Perhaps the first application of aluminium nitride for electronic applications was reported by Iwase and co-workers [10] who reported the use of AlN in the development of multilayer technology using thick-film gold, palladium–silver and copper systems. They reported good adhesion of thick-film systems (Au, Pd–Ag, Cu) to AlN when fired under the conditions similar to those for alumina substrates. Examination of the interface area revealed the presence of Pb, Cu, Si, and O [10, 11]. Werdecker and co-workers also discussed the possibility of utilizing aluminium nitride made by tape casting for electronic substrate applications [12, 13]. Characterization of substrates for surface roughness, camber, density, and contaminants in the substrate material was accompanied by thick- and thin-film metallizations, and a discussion of the difficulty of finding a co-fired system that can be fired in a nitrogen atmosphere. Evidence of continuing interest in metallization, co-firing, and performance of hybrid modules on AlN substrates is contained in a number of recent research papers [14–19].

3. Experimental procedure

3.1. Materials and processing

Aluminium nitride substrates were obtained from three different suppliers. One company (S1) supplied four different grades of commercially available aluminium nitride. The grades were designated by their approximate thermal conductivity in $\mathrm{W\,m^{-1}\,K^{-1}}$ (70, 130, 170 and 200). S2 and S3 represent substrates obtained from two other suppliers.

Two different gold thick-film paste systems (suppliers P1 and P2) were examined on the substrates from supplier S2. In addition, one palladium–silver conductor paste (supplier P2) and one ruthenium oxide resistor paste (supplier P2) were also examined on substrates from supplier S2. The gold thick-film pastes from vendor P1 were also examined on the substrates from vendor S3, and on all four grades of the substrates from vendor S1. Table I shows the various substrate/paste combinations examined in this study.

TABLE I Substrate–thick film ink combinations examined

Thick film pastes	Substrate					
	S1-70	S1-130	S1-170	S1-200	S2	S3
Gold (P1)	X^1	X	X	X^2	X^3	X^4
Gold (P2)					$X^{5,6}$	
Pd–Ag (P2)					X^7	
RuO (P2)					X^8	

S1 series: Toshiba–Norton
S2: Tokuyama–Soda
S3: Keramont
Superscript numbers indicate cross-section sample number.

The pastes were printed with a 325-mesh stainless steel screen with a 15-μm emulsion thickness and a 45° mesh angle. The thick-film material was allowed to level at room temperature and then dry for 10 min at 125 °C. Firing was done in an infrared furnace with air atmosphere and a peak temperature of 800 °C for 10 min. It was reported that the adhesion of the gold paste from supplier P2 degraded with repeated firings. Therefore, one sample of that paste on a substrate from supplier S2 was fired through the same profile a total of five times.

3.2. Materials characterization

A photograph of the gold metallization pattern on the six different substrates examined showed no obvious macroscopic abnormalities and the screen-printed patterns were free of blisters, holes or other gross defects.

For interface reaction studies, a section was cut out of each sample using a low-speed diamond-impregnated saw. Each section was then mounted in thermosetting epoxy mounting media perpendicular to the face of the sample for cross-sectional examination. Successive grinding steps were performed with 165-, 45- and 30-μm diamond grinding plates, and finish grinding was performed with 600-grit silicon carbide paper. The cross sections were then polished with 6- and 1-μm diamond paste.

Scanning electron microscopy, secondary electron imaging, Robinson backscattered electron imaging, energy dispersive spectroscopy, and microprobe analyses were utilized to characterize the interfaces of the various samples. Microchemical analyses were performed at different locations across the interface of each specimen.

4. Results and discussion

Metallized substrates examined by optical microscopy are shown in Fig. 1 (the Pd–Ag conductor pattern and

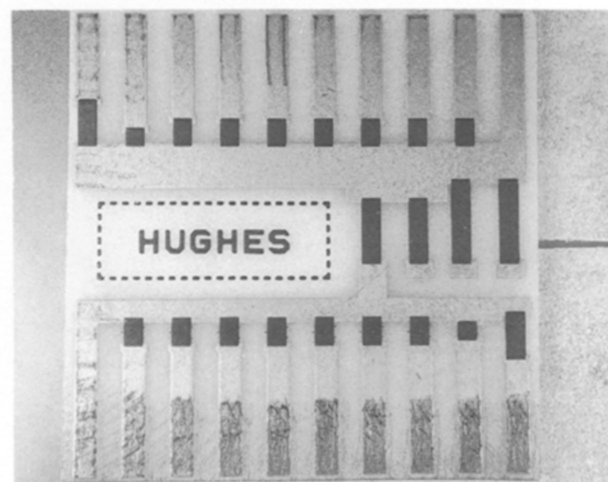

Figure 1 Palladium silver and ruthenium oxide resistor networks on aluminium nitride substrate.

RuO resistor pattern) and Fig. 2 (the gold metallization pattern). No macroscopic abnormalities were noted on any of the substrates by optical microscopy.

Four-point probe-resistivity measurements were taken on all of the gold metallization patterns using a Hewlett-Packard Model 3478A Multimeter with "autozero function" for the measurements in conjunction with an Alessi Industries four-point probe station. The data collected are included in Table II.

Optical microscopy also revealed a very thin layer of material at the metal–ceramic interface on all of the gold metallized specimens (Fig. 3). This layer was significantly thicker on sample 6 (Fig. 3b). Characterization by backscattered SEM revealed that higher atomic-number elements had diffused into the aluminium nitride. These data are substantiated by Fig. 4 which contains EDS traverses of the interfaces. A definite reaction zone (approximately 1.5 μm thick) is visible in the micrographs, and higher atomic-number elements have diffused to a distance slightly larger than suggested by the EDS data. This figure also shows that lead plays a major role in the adhesion reaction, and that Si, Ca, Cu, and Zn are present in significantly lesser amounts.

It is interesting to note that very little difference exists in the reaction between the various substrates and the same thick-film paste, with the exception of the substrate from S3. Sample 4 (substrate S3) had a reaction zone that was much thinner than the samples made with other substrates. The EDS data obtained from sample 4 seemed to indicate that the diffusion of lead, and possibly some of the other elements, had occurred further into the aluminium nitride than with the other samples. This could explain why relatively smaller amounts could be seen with backscattered electron detection (Fig. 5).

Examinations of samples 5 and 6 were performed similarly. Sample 5 was examined first where some marked differences were noted from the substrates with gold from vendor P1. A reaction zone was present, but much thinner than that found on the other substrates. Diffusion of the thick-film components into the grain boundaries of the aluminium nitride was noted (Fig. 6a and b) It was also noted that more of the binder phase stayed in the gold structure rather than diffusing to the interface (Fig. 6).

Fig. 6c and d are electron micrographs of sample 6. The most obvious characteristic noted (Fig. 6c) is the crack running along the interface which sometimes includes the first grain of substrate material. It was noted in other areas that this crack occurred for the most part at the reaction zone aluminium–nitride interface. It was also noted that this sample had a

TABLE II Resistivity measurements of gold conductors

Substrate	Paste type	R (Ω)	No. of pads	ρ (mΩ pad^{-1})
S2	ESL D8835-1D	1.102	250	4.4
S3	ESL D8835-1D	1.088	250	4.4
S1-70	ESL D8835-1D	1.285	250	5.1
S1-130	ESL D8835-1D	1.267	250	5.1
S1-170	ESL D8835-1D	1.313	250	5.3
S1-200	ESL D8835-1D	1.291	250	5.2
S2	Shoei 4460 (1 firing)	0.885	250	3.5
S2	Shoei 4460 (5 firings)	0.949	250	3.8

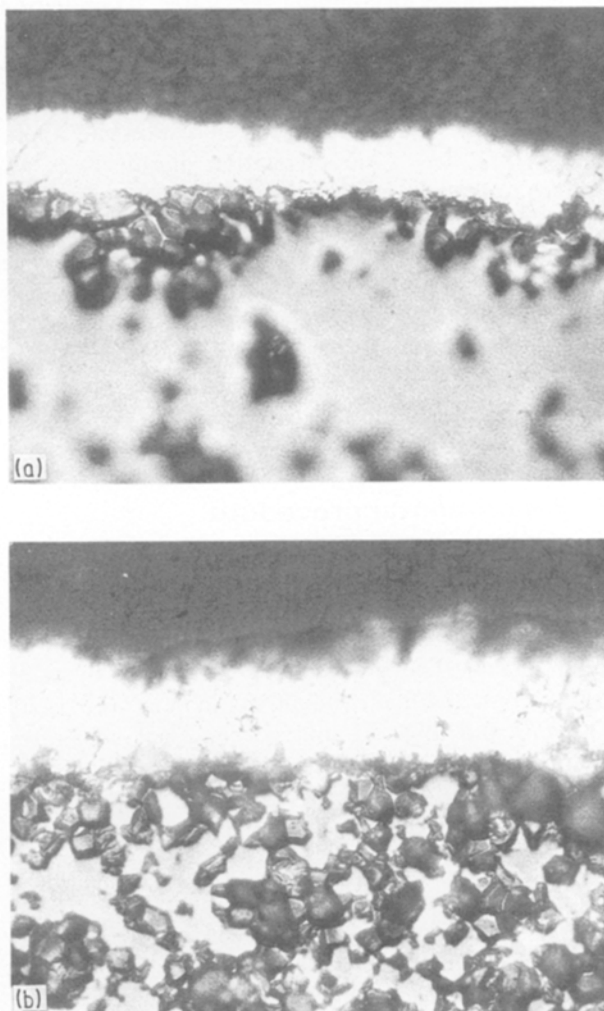

Figure 3 Light-field optical photomicrographs of gold–AlN interface in cross section. Samples (a) 3; (b) 6.

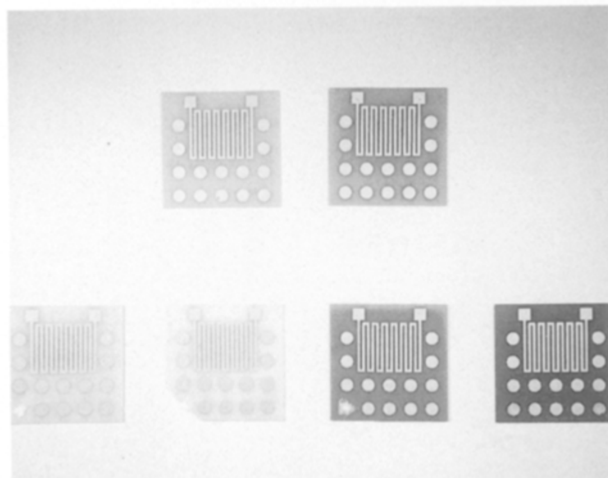

Figure 2 Gold thick-film patterns on various aluminium nitride substrates.

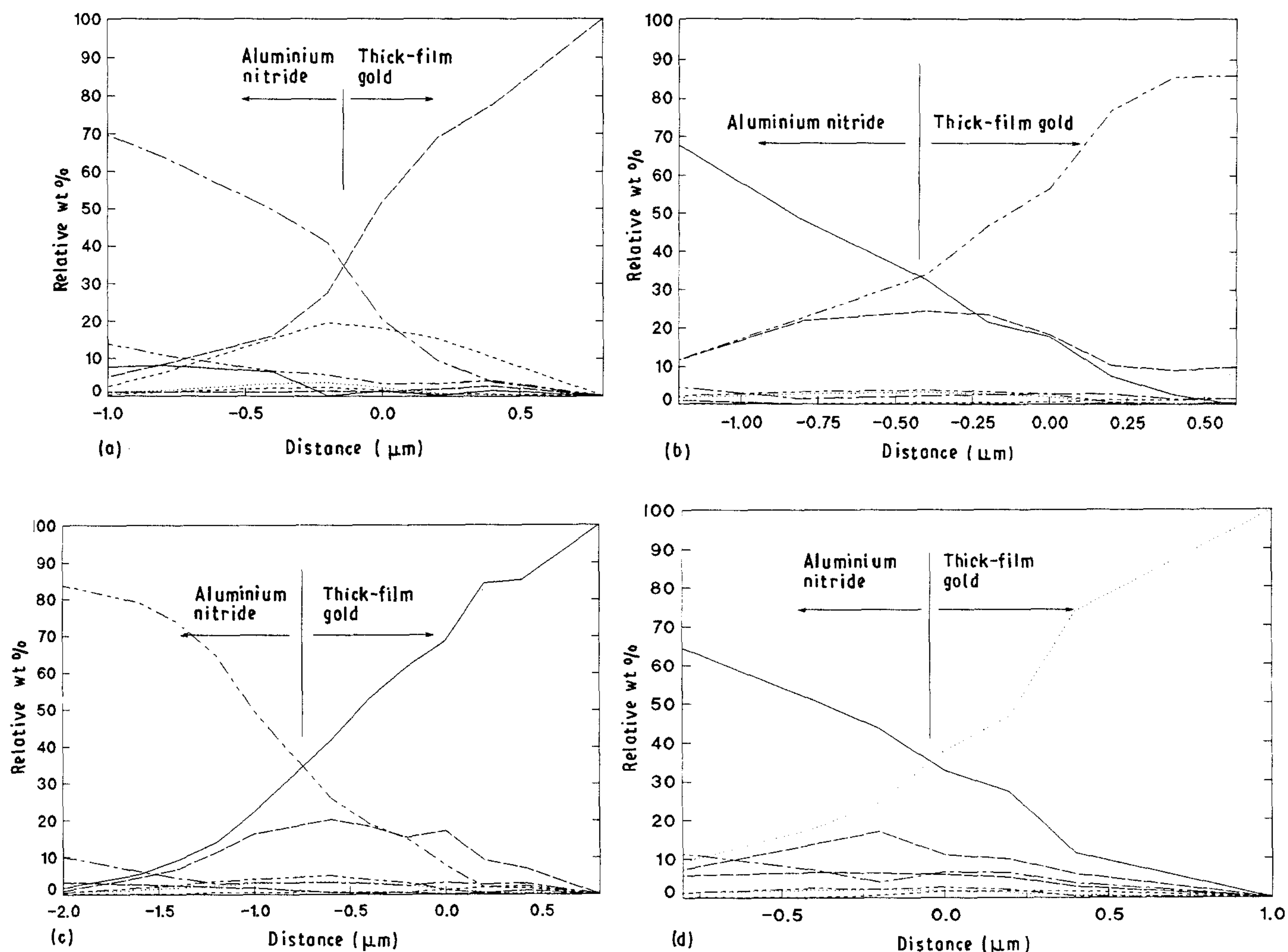

Figure 4 EDS data obtained from P1 gold–AlN interfaces. Samples (a) 1: Cd(-- –); Au(— —); Pb(----); Al(- —); Si(——); Ca(— —); Cu(----); Zn(·······) (b) 2: Al(——); Si(— —); Ca(----); Cu(·······); Zn(-- –); Cd(- —); Au(-- –); Pb(— —) (c) 3: Al(-- —); Si(— —); Ca(----); Cu(·······); Zn(-- –); Cd(- —); Au(——); Pb(— —) (d) 4: Al(——); Si(— —); Ca(----); Cu(·······); Zn(-- –); Cd(- —); Au(·······); Pb(— —).

fairly thick reaction zone. EDS data (Fig. 7b) confirmed the thick reaction zone, but also showed that very little diffusion of the other elements into the aluminium nitride had occurred at this location. The EDS traverse indicated that a thick layer of material with a fairly constant proportion of aluminium and gold had formed. In addition, a very wide band of material had lead present in large quantities. It was also noted that a significant amount of silicon was found near the aluminium–nitride reaction-zone interface. Fig. 6c indicates that a large number of islands of binder material formed in the thick-film material. These islands were significantly smaller in the other sample (No. 5), and absent in the other gold (supplier P1) samples.

Several elements were found in the thick-film gold from P1 that were not found in the gold samples from P2. Cadmium, calcium, and copper were absent in the EDS traverses of the samples from P2. However, trace amounts of copper were found in the islands that had formed in the P2 thick-film material. This might indicate that the cadmium (which was found in significant quantities in the P1 samples), and possibly calcium, act to prevent the other elements in the binder from diffusing rapidly into the grain boundaries and from coalescing into islands within the thick-film material.

Examination of the palladium silver sample with optical and scanning electron microscopy indicated that a thin layer of material exists between the metal layer and the aluminium nitride substrate. EDS indicated (Fig. 8a) that this layer was high in chromium, with a high proportion of bismuth at the interface of this layer with both the ceramic and the metal. EDS also indicated that lead was present and was associated with the ceramic side of the interface. Both the micrographs and the EDS traverse indicate that this reaction zone is approximately 3 μm in width.

The ruthenium oxide–resistor interface was less obvious than the Pd–Ag interface. Light-field optical, polarized optical and scanning electron microscopy showed no obvious reaction zone at the resistor–AlN interface (Fig. 9b). However, EDS indicated that elements from the resistor paste did diffuse into the aluminium nitride. Fig. 8b shows the data, in which diffusion of Ru, Zn, Ca, and Ti can be seen ~ 8 μm into the AlN. In addition, a small amount of K and Mn can also be seen at this interface.

5. Summary and conclusions

Aluminium nitride was successfully metallized using standard screen-printing apparatus and thick-film

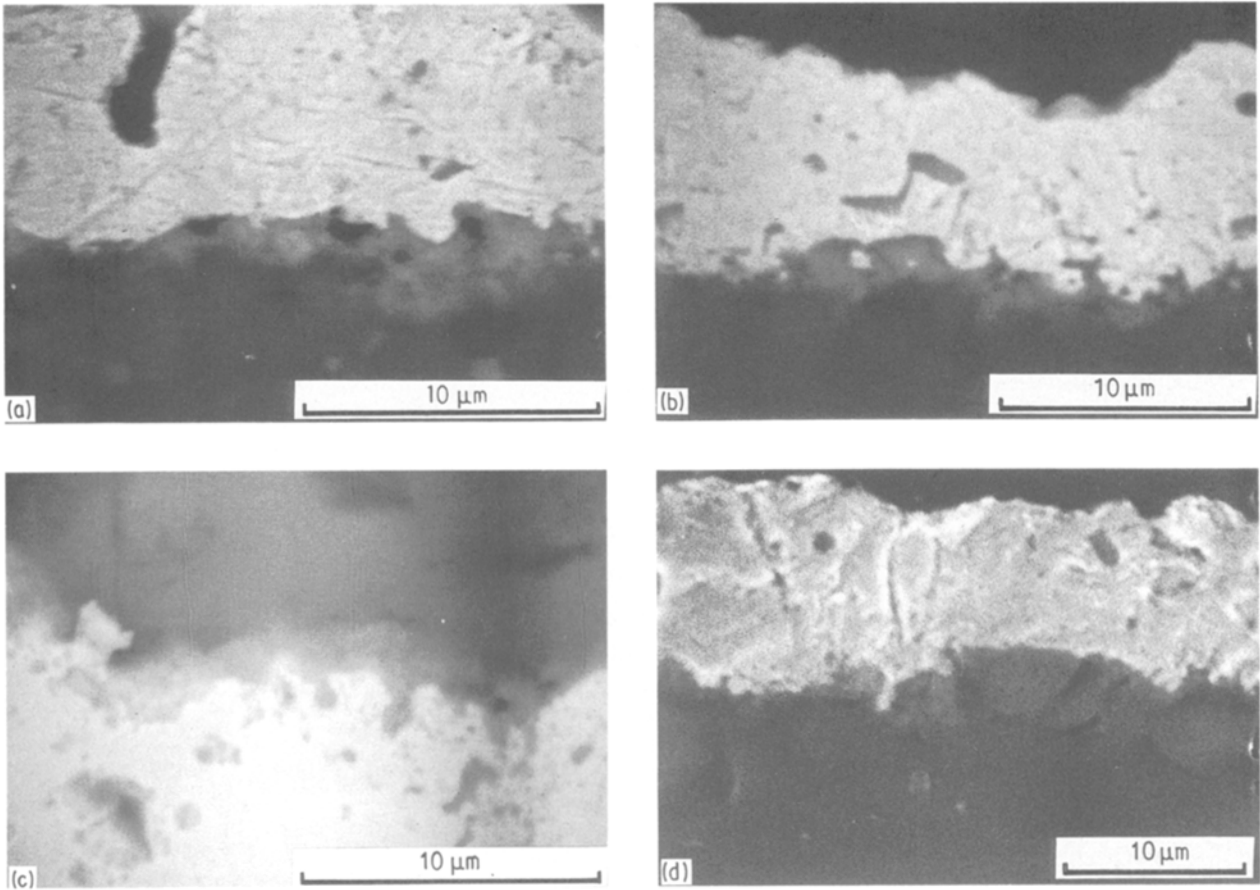

Figure 5 Backscattered SEM of P1 gold–AlN interfaces in cross section. Samples (a) 1; (b) 2; (c) 3; (d) 4.

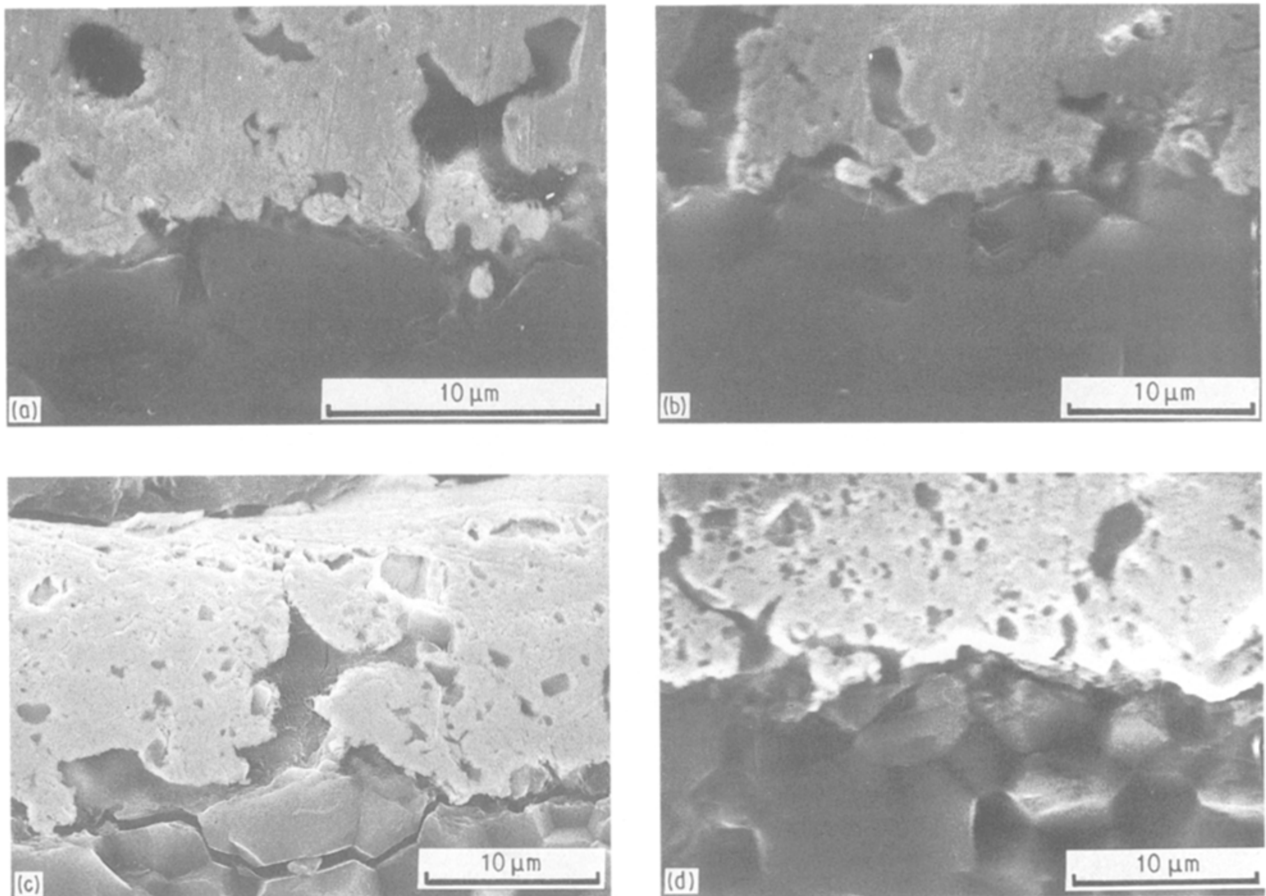

Figure 6 SEM of P2 gold–AlN interfaces showing the difference between 1 and 5 firings of the same ink. (a) Secondary electron image of sample 5; (b) backscattered electron image of sample 5; (c) secondary electron image of sample 6; (d) backscattered electron image of sample 6.

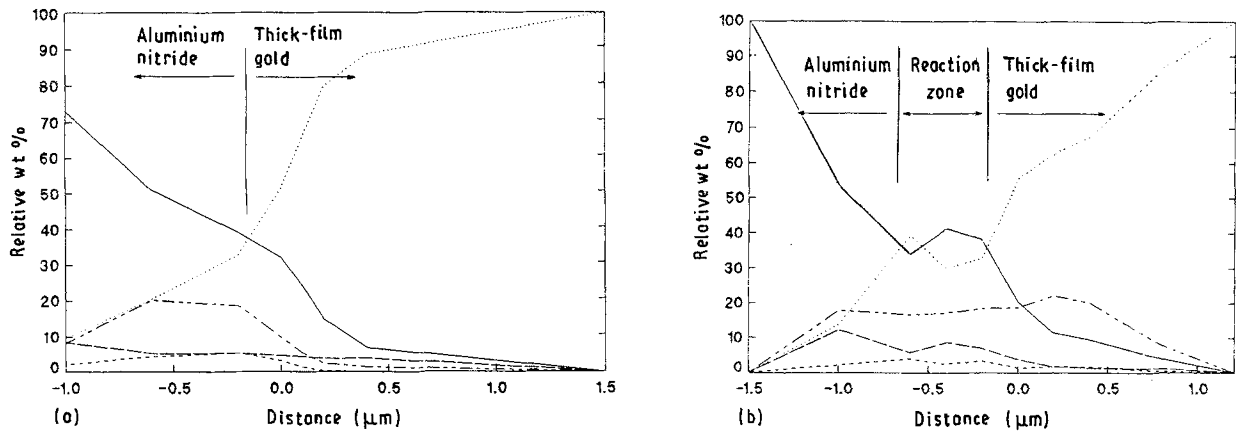

Figure 7 EDS data obtained from P2 gold–AlN interfaces. Contrasting difference between 1 and 5 firings of the same ink. Samples (a) 5: Al(——-); Si(– – –); Zn(--------); Au(·······); Pb(-- – -- –) (b) 6: Al(———); Si(– – –); Zn(--------); Au(·······); Pb(- – -- –).

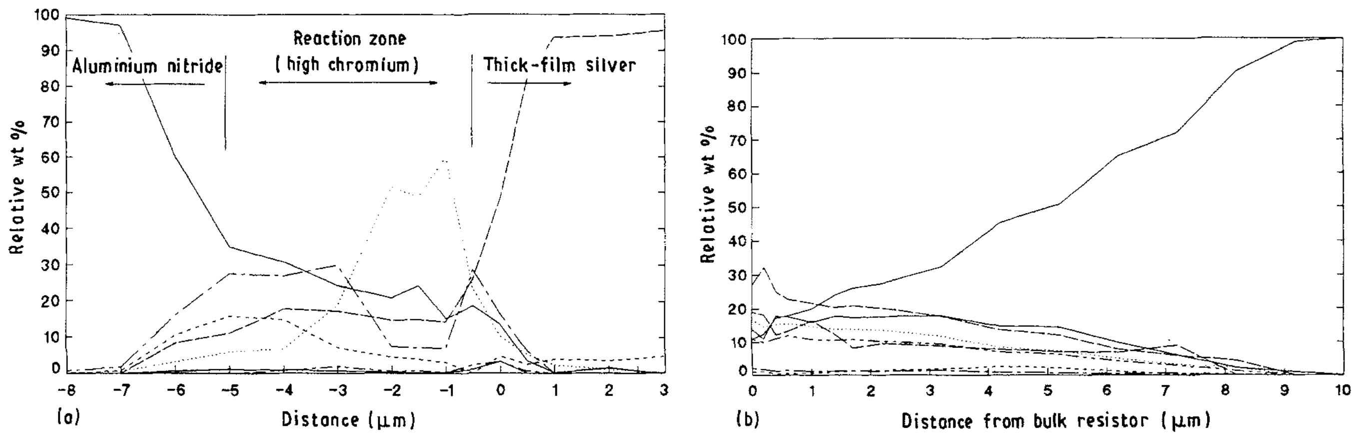

Figure 8 EDS data from palladium silver conductor–AlN and ruthenium oxide resistor–AlN interfaces. Samples (a) 7 (Pd–Ag): Al(——); Ag(— —); Pb(----); Cr(·······); Si(-–-); Bi(- —); Ca(——) (b) 8 (RuO): Al(——); Si(— —); K(----); Ca(·······); Ti(-- -); Mn(- —); Zn(——); Ru(— —).

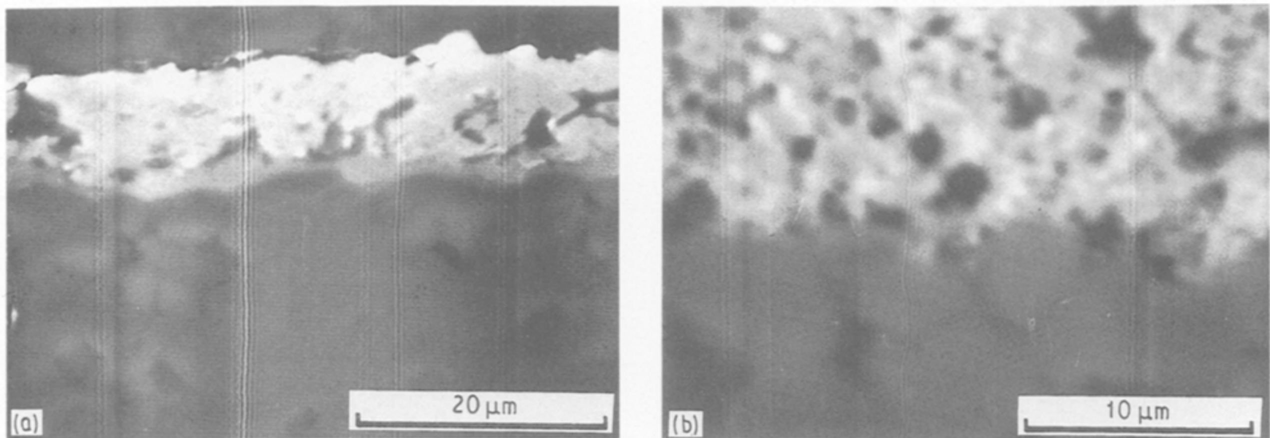

Figure 9 Backscattered electron images of palladium silver conductor–AlN and ruthenium oxide resistor–AlN interfaces. Samples (a) 7 (Pd–Ag); (b) 8 (RuO).

inks. Interface analyses reveal that the binder material in one type of palladium silver thick film paste consists of chromium, bismuth, lead, silicon, and calcium, while the binder material in the thick-film gold pastes consist of lead, silicon and copper, with traces of cadmium, calcium and zinc. The elements that make up the binder migrate to the interface of the metal and ceramic, most probably in the form of amorphous oxides. These glassy phases react with the ceramic, thus assisting in the adhesion of the thick-film material. Repeated firing degraded the adhesion of gold thick-film systems that did not contain cadmium, zinc and calcium. One or more of these elements hold the major elements (lead, silicon, bismuth) in a glassy phase and prevent substantial migration into the aluminium nitride grains.

Acknowledgements
This work is based on C. E. N.'s MSc thesis and was partially supported by the Hughes Corporation.

References
1. R. R. TUMMALA and E. J. RYMASZEWSKI, Microelectronics Packaging Handbook (Van Nostrand-Reinhold, 1989) pp. 492–510.
2. N. KURAMOTO, H. TANIGUCHI and I. ASO, *Amer. Ceram. Soc. Bull.* **68** (1989) 883.
3. L. M. SHEPPARD, *ibid.* **69** (1990) 1801.
4. N. IWASE, A. TSUGE and Y. SUGIURA, *Int. J. Hybrid Microelectron.* **7** (1984) 49.
5. K. KOMEYA, A. TSUGE, H. INQUE and H. OTHA, *Yogyo-Kyokai-Shi* **89** (1981) 58.
6. K. SHINOZAKI, K. ANZAI, T. TAKANO, A. TSUGE and K. KOMEYA, in Proceedings of the 22nd Symposium on Basic Science of Ceramics, Yogyo-Kyokai, January 1984, p. 43.
7. L. MAYA, *Adv. Ceram. Mater.* **1** (1986) 150.
8. E. K. BEAUCHAMP, M. J. CARR and R. H. GRAHAM, *ibid.* **2** (1987) 79.
9. Y. KUROKAWA, K. UTSUMI and H. TAKAMIZAWA, *J. Amer. Ceram. Soc.* **71** (1988) 588.
10. N. IWASE, K. ANZAI, K. SHINOZAKI, O. HIRAO, T. D. THANH and Y. SUGIURA, *IEEE Trans. CHMT* **8** (1985) 253.
11. N. IWASE, K. ANZAI and K. SHINOZAKI, *Solid State Tech.* **29** (1986) 135.
12. W. WERDECKER and F. ALDINGER, in Proceedings of the ECC, May 1984, pp. 402–6.
13. W. WERDECKER and F. ALDINGER, in Proceedings of the 35th Electronic Components Conference, 1985, p. 26.
14. S. G. KONSOWSKI, J. A. OLENICK and R. D. HALL, in Proceedings of the International Symposium on Microelectronics, November 1985, p. 213.
15. A. A. MOHAMMED and S. J. CORBETT, *ibid.* p. 218.
16. N. KURAMOTO, H. TANIGUCHI and I. ASO, *IEEE Trans. Components, Hybrids, Manuf. Tech.* (1986) pp. 424–29.
17. N. IWASE, T. YNAZAWA, M. NAKAHASHI, K. SHINOZAKI, A. TSUGE and K. ANZAI, in Proceedings of the 37th IEEE Electronic Components Conference, 1987, pp. 384–391.
18. E. S. DETTMER and H. K. CHARLES, *J. Hybrid Microelectron.* **10** (1987).
19. E. S. DETTMER and H. K. CHARLES, in Proceedings of the International Society for Hybrid Microelectronics, November 1987, p. 19.

Received 21 November 1990
and accepted 10 April 1991